THE ASTROPHYSICAL JOURNAL, 491:L77–L80, 1997 December 20

DETECTION OF EXTENDED OPTICAL EMISSION ASSOCIATED WITH THE NORTHERN RADIO HOT SPOT OF 3C 390.3

M. ALMUDENA PRIETO
Instituto de Astrofisica de Canarias, Via Lactea, E-38200 La Laguna, Tenerife, Canary Islands, Spain; aprieto@iac.es
AND
JARI K. KOTILAINEN[1]
International School for Advanced Studies (SISSA), via Beirut 2-4, I-34014 Trieste, Italy; jkotilai@sissa.it
Received 1997 August 15; accepted 1997 October 8; published November 11

ABSTRACT

We present deep *V*, *R*, and *I* broadband CCD images of the northern radio lobe associated with the radio galaxy 3C 390.3. Spatially resolved emission coincident with the brightest region of the northern lobe (hot spot B) is detected in all filters, with surface brightness $V = 24.6$ mag arcsec^{-2} and $V - I$ color ~ 0.8. The new optical data, together with the available radio and X-ray data for the hot spot, are compatible with a straight synchrotron spectrum of power-law index ~ -0.8. The source of optical emission is extended, and its shape and size are in good agreement with those seen at radio wavelengths. The second brightest region in the northern lobe (head A) was not detected in any of the filters. The upper limit to its brightness is $I \sim 23$ mag.

Subject heading: galaxies: individual (3C 390.3) — radiation mechanisms: nonthermal — radio continuum: galaxies

1. INTRODUCTION

Radio hot spots are relatively common in extragalactic, lobe-dominated radio sources. Although the search for their counterpart optical emission has a long history (e.g., Simkin 1978; Crane, Tyson, & Saslaw 1983), so far only a few have been clearly detected as sources of optical waves. Indeed, at high frequencies, most well-studied hot spots show an abrupt steepening of the spectrum below that extrapolated from the lower frequency power law, which is widely interpreted as the result of a high-energy cutoff in the particle distribution of the synchrotron spectrum. This is clearly illustrated by the hot spots associated with 3C 247, 3C 273, and 3C 33 (Keel & Martini 1995; Röser & Meisenheimer 1986; Meisenheimer & Röser 1986), all showing a high-frequency cutoff at $\sim 10^{14}$ Hz. So far, there are only two reported cases in which the hot spot synchrotron spectrum decays smoothly from radio to the UV, in 3C 303 (Keel 1988), or even to the X-rays, in 3C 390.3 (Prieto 1997). The western hot spot of Pictor A was also previously believed to exhibit a straight synchrotron spectrum extending to the X-rays (Röser & Meisenheimer 1987). However, recent new photometry by Meisenheimer, Yates, & Röser (1997) reveals Pictor A west exhibiting the typical optical spectra turnover that characterizes most hot spots.

The radio galaxy 3C 390.3 is an N-type elliptical galaxy at redshift $z = 0.0561$ (Osterbrock, Koski, & Phillips 1975). At this redshift, 1″ corresponds to ~1.5 kpc, assuming a Hubble constant $H_0 = 50$ km s^{-1} Mpc^{-1}. In radio, 3C 390.3 has a classical double-lobe morphology, the northern lobe being at a projected distance from the core of ~120″ (~180 kpc), and the southern lobe at ~87″ (~130 kpc). The brightest region in the northern lobe is identified as the hot spot B that is at a distance of ~140 kpc from the core (the nomenclature by Alexander 1985 is followed); the second brightest region is the tip of the lobe, identified as head A. Leahy & Perley (1995) discovered a faint, well-collimated thin jet that connects the core to the northern lobe, entering the lobe through the hot spot B. VLBI observations at 5 GHz show evidence of superluminal motion in the parsec-scale jet toward the northern lobe (Alef et al. 1996).

Prieto (1997) detected spatially resolved X-ray emission at the location of the northern lobe, for which the multiwavelength spectrum from radio to X-rays indicated a smoothly decaying synchrotron spectrum with a spectral index of -0.9. This Letter presents unambiguous evidence for the optical detection of the northern hot spot B of 3C 390.3, which provides further support for the smooth decay of the synchrotron spectrum beyond the optical range.

2. OBSERVATIONS

Broadband images in *V* (5460 Å), *R* (6660 Å), and *I* (7850 Å) filters of the field of the northern lobe of 3C 390.3 were obtained using the BroCam1 1024 pixel^2 CCD camera located at the Cassegrain focus of the 2.5 m Nordic Optical Telescope on La Palma, during the nights of 1996 July 18–20. The pixel scale of the images is 0.″176 pixel^{-1}, giving a field of view of 3.0 arcmin^2. Conditions were photometric, with seeing measured from field stars varying between ~0.″8 in *I* and ~1.″2 in *V*. Total integration times were 80, 90, and 80 minutes in the *V*, *R*, and *I* filters, respectively. Those consist of several 20 minute exposures that were co-added to remove cosmic-ray events and to increase the signal-to-noise ratio. To produce the final images, multiple exposures were co-added after accurate alignment to within a fraction of a pixel using field stars as reference points. Photometry was calibrated against faint standard star fields selected from Landolt (1992) that were observed frequently throughout the nights.

3. RESULTS

Figure 1 shows the 45″ × 45″ (~67 × 67 kpc) region centered on the northern radio lobe of 3C 390.3 in the *I*, *R*, and *V* bands, respectively. At low Galactic latitude, this region is very crowded, and a number of the bright stars in the field could be identified in the Palomar plates and their coordinates derived with COSMOS. Thus, the positions of the two out-

[1] On leave from Tuorla Observatory, Turku University, Väisäläntie 20 FIN-21500, Piikkiö, Finland.

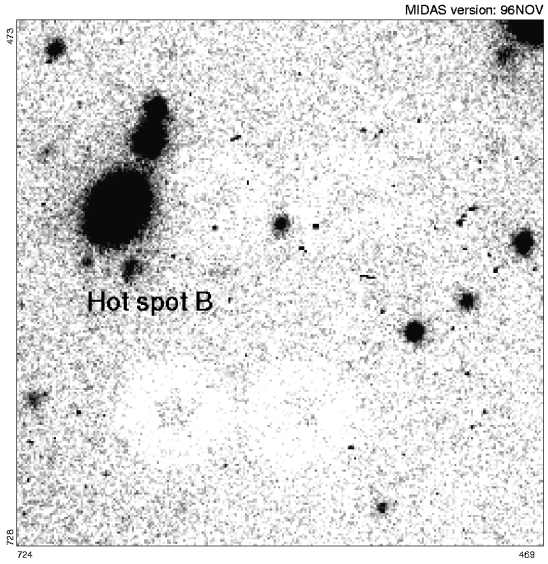

FIG. 1*a*

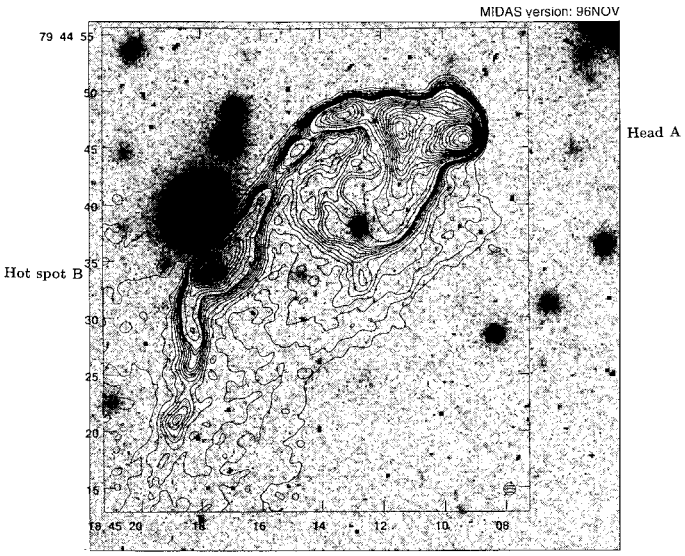

FIG. 1*b*

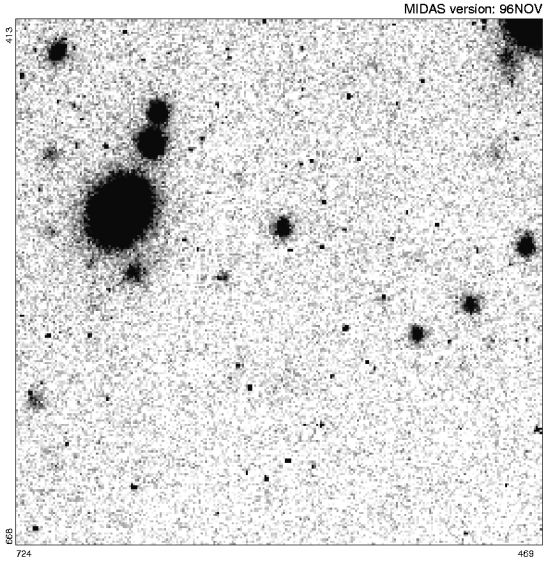

FIG. 1*c*

FIG. 1.—(*a*) *I*-band image of the field of the 3C 390.3 northern radio lobe. North is up, and east is to the left. The scale is 0.″176 pixel^{-1}, the size of the image is 45″ × 45″ (~67 × 67 kpc), and seeing is 0.″8 FWHM. The optical counterpart to the hot spot B is marked in the figure. The white rings in the image are artifacts. (*b*) Same as (*a*), but in the *R* band, and seeing is FWHM ~ 1″. The 18 cm radio map of the northern lobe with 1.″1 circular beam resolution (Leahy & Perley 1995) is overlaid on the image with contours. The positions of the hot spot B and the head A in the radio map are marked. (*c*) Same as (*a*), but in the *V* band, and seeing is FWHM ~ 1.″2.

standing features in the northern lobe, namely, the primary hot spot B and the head A, could be securely deduced based on astrometry from the surrounding field stars.

Figure 1*b* shows the 18 cm radio map of the northern lobe by Leahy & Perley (1995) overlaid on the *R*-band image. Both radio and optical images have comparable spatial resolution: the circular beam size of the radio image and the FWHM of the stars in the *R*-band image is ~1″ in both cases. The hot spot B in the map of Leahy & Perley falls exactly on the position of a faint extended source seen at all three optical wavelengths. On the other hand, the head A does not have a detectable optical counterpart in any of the filters.

The optical counterpart of the hot spot B is spatially resolved in all bands and has a diffuse, slightly curved morphology. This is most clearly seen in the *I*-band image (Fig. 1*a*), which has both the highest signal-to-noise ratio and the best spatial resolution (FWHM ~ 0.″8). An *I*-band contour plot of a 3.″5 × 3.″5 (~5.2 × 5.2 kpc) region centered on the hot spot B is shown in Figure 2*a*, with the lowest contour plotted at a 3 σ level above the sky background. For comparison, a contour plot of a nearby field star is shown in Figure 2*b*. Figure 2*a* shows the asymmetric morphology of the optical emission region. The overall structure is elongated, extending to ~2″ (~3 kpc) along its major axis, coinciding with the major axis of the counterpart radio structure. The *V* image has the worse seeing, and therefore the multiple structure seen in the *I* image is poorly seen in *V*. Nevertheless, the region is also extended in *V* with a FWHM of about 1.″6.

Integrated *V*-, *R*-, and *I*-band magnitudes in a 2″ diameter aperture centered on the hot spot B are given in Table 1. The

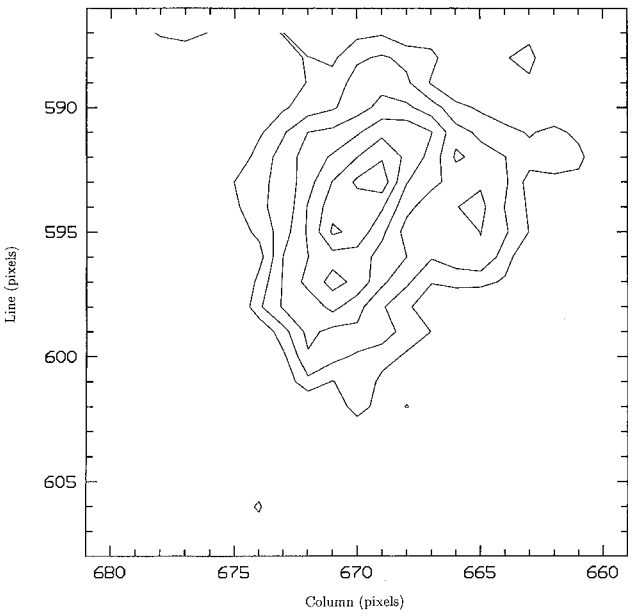

FIG. 2*a*

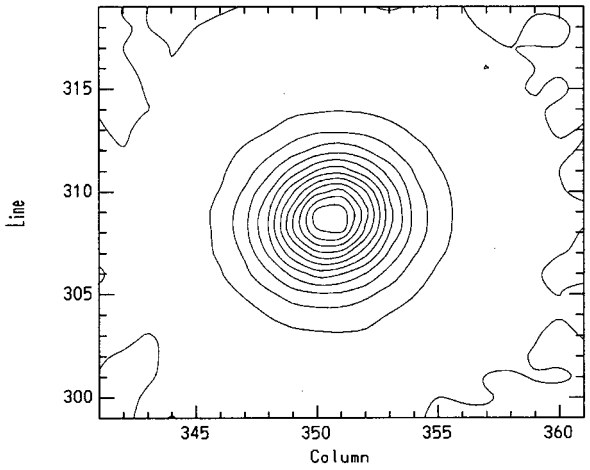

FIG. 2*b*

FIG. 2.—(*a*) *I*-band contour plot of the 3″.5 × 3″.5 (~5.2 × 5.2 kpc) region centered on the hot spot B. The lowest contour is at a 3 σ level (0.03 counts s^{-1} $pixel^{-1}$). The contours are separated by 1 σ intervals. The pixel scale is 0″.176 $pixel^{-1}$, and seeing is FWHM = 0″.8 [see (*b*)]. (*b*) *I*-band contour plot of a nearby field star. The highest contour corresponds to the peak of the emission, ~3.8 counts s^{-1} $pixel^{-1}$. The contours are separated by 15 σ intervals (~0.4 counts s^{-1} $pixel^{-1}$). The pixel scale is 0″.176 $pixel^{-1}$, and the measured FWHM = 0″.8.

head A was not detected in any filter, and we estimate its brightness to be $I \geq \sim 23$ mag, the limiting magnitude of the *I*-band image. Saslaw, Tyson, & Crane (1978) provided the first tentative optical identification of the northern field on the basis of photographic plates. The bright source identified with the hot spot B in our images was detected at the confusion level in their plates (cf. their Fig. 6). They estimated the surface brightness of the source (identified as 17.7) to be $B \sim 25$ mag $arcsec^{-2}$. We derive a slightly brighter value of $V \sim 24.6$ mag $arcsec^{-2}$ within a 2″ aperture[2].

Figure 3 shows the currently available multifrequency spectrum for the hot spot B. The 5 GHz fluxes are from Leahy & Perley (1995), measured in a 1″ aperture, and from Hargrave & McEllin (1975), measured in a 2″.2 × 1″ aperture, both centered on the peak position of hot spot B. Measurements at 0.6 and 1.4 GHz are from Jägers & Ma (1984) and correspond to a beam resolution of 30″. These latter data may include an important contribution from the background lobe emission, and they are plotted only for comparative purposes. The optical data are from this work and correspond to integrated fluxes in a 2″ diameter aperture, corrected for Galactic extinction [$N(H) \sim 0.4 \times 10^{21}$ cm^{-2}; Dickey & Lockman 1990). The X-ray data are from Prieto (1997).

It is apparent from Figure 3 that the overall radio-to-optical spectrum does not show the typical spectral turnover at $\sim 10^{14}$ Hz seen in most hot spot spectra but instead shows a smooth decay toward high frequencies. Such a behavior indicates that any high-frequency cutoff in the synchrotron spectrum has to occur at higher frequencies than the optical. On the other hand, an extrapolation of the radio-to-optical spectrum to the X-rays is consistent with the measured *ROSAT* flux at the northern lobe position.

Power-law spectral indices derived on the basis of the 5 GHz and optical fluxes give an average value $\alpha_{(r-o)} \sim -0.8$, whereas in the much shorter *I*-to-*V* range, the spectral index becomes steeper, $\alpha_{(V-I)} \sim -1.2$. The uncertainties inherent in the optical measurements affect more dramatically the shape of the shorter *I*-to-*V* band range, hence most likely causing the difference in

[2] Keel & Martini (1995) give a foreground K4 star as the most prominent candidate for the hot spot B. However, the position of this source falls clearly outside the northern radio lobe in the map of Leahy & Perley (1995).

TABLE 1

MAGNITUDES OF HOT SPOT B OF 3C 390.3

Band	Magnitude
V	23.3 ± 0.4
R	22.8 ± 0.3
I	22.1 ± 0.4

NOTE.—Magnitudes are derived in a 2″ diameter aperture.

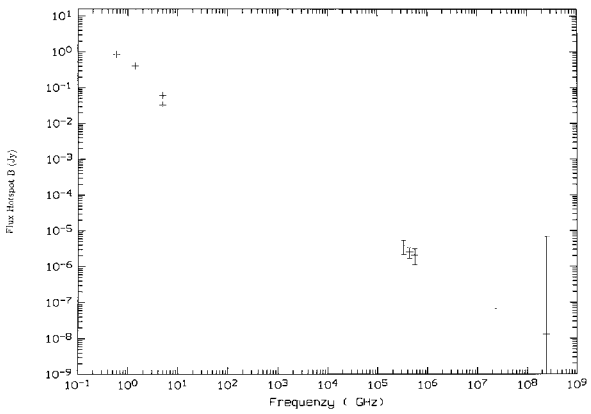

FIG. 3.—Currently available multifrequency spectrum of the 3C390.3 hot spot B. See text for sources.

the spectral index. Yet, the smooth steepening of the optical spectrum toward the red is clearly apparent from Figure 3 and is in agreement with the general continuum trend.

4. DISCUSSION

Multiwavelength studies of several well-known hot spots clearly support the synchrotron nature of their spectra, usually characterized by a power-law spectral index of $\alpha \sim -0.5$ in the low-frequency range and a high-frequency cutoff occurring somewhere below $\sim 10^{14}$ Hz. The primary hot spot B at the northern lobe of 3C 390.3, however, exhibits a smooth, straight synchrotron spectrum down to the optical frequencies. The other known case of a hot spot with a similar spectrum is 3C 303 west. Both show similar radio-to-optical spectral indices, -0.95 in 3C 303 (Röser 1988) and -0.83 in 3C 390.3 (this work), that contrast with the wider and flatter range seen in most hot spots, typically covering the $0.5 < \alpha < 1.0$ range.

Spatially resolved hot spots often have asymmetric morphologies in the radio; however, they have so far rarely been resolved at optical wavelengths. Recent *Hubble Space Telescope*/Faint Object Camera imaging of Pictor A west (Thomson, Crane, & Mackay 1995) resolves the region in a series of wisps elongated perpendicular to the radio jet, all over covering about 1.″4 (~1 kpc) in size. In the case of 3C 303 west, the optical counterpart is barely elongated along the line toward the nucleus of 3C 303 (Keel 1988). Finally, in the case of 3C 390.3, the hot spot B is resolved in our three optical images. Its structure is elongated in the same direction as the radio-emitting region. In this direction, the size of the optical region at a 3 σ level (Fig. 2*a*) is ~2″ (~3 kpc), and ~1.″5 (~2 kpc) in the perpendicular direction.

The radio emission associated with 3C 390.3 northern hot spot B is elongated in the direction of the faint radio jet connecting the core and the hot spot B, and its size, estimated from the 6 cm radio map of Leahy & Perley (1995, their Fig. 12*a*) is ~9.″0 × 1.″3 (~3.0 × 2.0 kpc), in perfect agreement with the optical dimensions. The radio emission shows a peak with FWHM ~ 0.″6; the optical emission also shows a peak at an 8 σ level (cf. Fig. 2*a*), although it is unresolved at the 0.″8 spatial resolution of our data. The higher spatial resolution of the 6 cm image (0.″33) hampers any detailed comparison with the optical image, thus, although presumably related, the relative position of both peaks in the hot spot region is uncertain. Finally, both optical and radio emission show marginal extended structure at a location roughly to the west of the peak position. This secondary extended emission, which is clearly seen in the radio image, is just outlined in the optical image (cf. Fig. 2*a*). In summary, the overall morphology of the optical- and radio-emitting regions is very similar in shape and size, which provides further support for the synchrotron nature of the optical emission.

The northern hot spot B in 3C 390.3 adds a new case to the rare class of hot spots with straight synchrotron spectrum beyond the optical frequencies. We are thus witnessing the production of energetic particles with Lorentz factors larger than 10^6 at a distance from the core of 3C 390.3 of ~140 kpc. Using Prieto's (1997) values, the estimated magnetic field in B is ~10 nT, and the acceleration timescale for the optical electrons is ~500 yr. This is a factor ~10 shorter than the light-travel time across the diameter of the optical region. Thus, unless particles are transported loss free, reacceleration must be occurring at different points along the hot spot region. In that sense, the general morphological agreement between the optical- and radio-emitting regions is enlightening.

REFERENCES

Alef, W., Wu, S. Y., Preuss, E., Kellermann, K. I., & Qiu, Y. H. 1996, A&A, 308, 376
Alexander, P. 1985, MNRAS, 213, 743
Crane, P., Tyson, J. A., & Saslaw, W. C. 1983, ApJ, 265, 681
Dickey, J. M., & Lockman, F. J. 1990, ARA&A, 28, 215
Hargrave, P. J., & McEllin, M. 1975, MNRAS, 173, 37
Jägers, W. J., & Ma, E. 1984, Chinese Astron. Astrophys., 8, 140
Keel, W. C. 1988, ApJ, 329, 532
Keel, W. C., & Martini, P. 1995, AJ, 109, 2305
Landolt, A. 1992, AJ, 104, 340
Leahy, J. P., & Perley, R. A. 1995, MNRAS, 277, 1097
Meisenheimer, K., & Röser, H.-J. 1986, Nature, 319, 459
Meisenheimer, K., Yates, M. G., & Röser, H.-J. 1997, A&A, 325, 57
Osterbrock, D. E., Koski, A. T., & Phillips, M. M. 1975, ApJ, 197, L41
Prieto, M. A. 1997, MNRAS, 284, 627
Röser, H.-J. 1988, in Hot Spots in Extragalactic Radio Sources, ed. K. Meisenheimer & H.-J. Röser (Berlin: Springer), 91
Röser, H.-J., & Meisenheimer, K. 1986, A&A, 156, 15
———. 1987, ApJ, 314, 70
Saslaw, W. G., Tyson, J. A., & Crane, P. 1978, ApJ, 222, 435
Simkin, S. 1978, ApJ, 222, L55
Thomson, R. C., Crane, P., & Mackay, C. D. 1995, ApJ, 446, L93